Impact of Small Regenerator Structural Flaws on the Performance of Miniature Pulse Tube Cryocoolers

T.J. Conrad[1], S.M. Ghiaasiaan[1], C.S. Kirkconnell[2], T. Crittenden[3]

[1]Georgia Institute of Technology, Atlanta, GA 30332 USA
[2]Iris Technology Corporation, Irvine, CA USA
[3]Virtual AeroSurface Technologies, Atlanta, GA USA

ABSTRACT

Miniature cryocoolers are suitable for space applications and installation in portable devices. They can also be useful as final stages for applications where small cooling loads must be carried at temperatures lower than that required by the primary load. Strong regeneration, near plug-flow regime in the pulse tube and good flow control are essential for these cryocoolers to function.

Miniature cryocoolers that use wire mesh as regenerator filler generally have a much larger ratio of regenerator filler pore size to regenerator diameter than their larger counterparts. For this reason, the significance of gaps existing between the porous regenerator filler and the interior wall of the regenerator shell will likely be greater for miniature cryocoolers. These gaps provide a low resistance flow path which may decrease the effectiveness of the regenerator. In this investigation the effects of such gaps on the performance of miniature pulse tube cryocoolers are examined using 2-D CFD simulations. Miniature scale pulse tube cryocooler designs whose suitability for cooling under ideal conditions that have been theoretically demonstrated are used as the basis for this study. The results confirm that extra precision and robustness are needed for miniature cryocoolers.

INTRODUCTION

Miniature scale Pulse Tube cryocoolers (PTCs) have been a subject of intense research interest for some time[1-4] and have recently begun to be practically demonstrated[5]. Such cryocoolers are attractive due to their minimal size and weight for space applications and portable devices. Miniature coolers might also be useful as final stages for applications where small cooling loads must be carried at temperatures lower than that required by the primary load. In such an application, a larger cryocooler might carry the primary load while the miniature stages carry the smaller, colder ones, improving the overall efficiency of the cooling system.

Further development of miniature PTCs from laboratory demonstrations to usable devices is likely to require modeling and analysis techniques which may be different from those used for larger cryocoolers. Certainly, some of the phenomena affecting the performance of miniature PTCs are likely to differ from those that are dominant at larger scales. The regenerator defects addressed in this paper are one example of such phenomena, which is generally not considered when modeling conventional scale cryocoolers.

Cryocoolers 16, edited by S.D. Miller and R.G. Ross, Jr.

Due partially to limitations on the wire and pore diameters of available wire mesh screens, miniature cryocoolers that use these materials as regenerator fillers generally have a much larger ratio of regenerator filler pore size to regenerator diameter than their conventionally sized counterparts. The porous morphology of the screens prevents them from being cut to perfectly match the diameter of the regenerator housing. Magnified photographs of punched #635 mesh stainless steel screens, presented in Figure 1, show that the edge of a cut screen will consist of partial mesh cells which have a characteristic size less than or equal to the pore diameter. As a result of both this irregular edge and manufacturing considerations, some open space is expected to exist between the edges of the screens and the housing with a size that is likely on the order of the mesh screen pore diameter. These gaps provide a low resistance flow path which may decrease the effectiveness of the regenerator. Because the pore diameter will be larger in relation to the regenerator diameter for miniature PTCs, the effects of these gaps on the performance of the miniature coolers will likely be more significant as well.

Because of such unique considerations, the applicability of currently existing analytical tools to the design of miniature PTRs is uncertain. Even the most advanced design tools[6-7] are typically one-dimensional and rely on constitutive and closure relations that are at best approximations for the complex and periodic flow conditions in PTRs. As PTRs are miniaturized, it is expected that multidimensional flow effects and detailed prediction of thermal-hydraulic flow phenomena, particularly in the regenerator, will become even more important, requiring models able to accurately represent these flow details.

In this investigation, the effects of gaps between the filler matrix and regenerator wall of a miniature pulse tube cryocooler on its performance were examined using 2-D CFD simulations with the Fluent CFD package[8]. Recent successful simulations of cryocooler systems using CFD tools[1, 9-10] have shown that such models can provide useful performance predictions for pulse tube refrigerators. Commercial CFD packages such as Fluent have been shown to be capable of detailed solutions of models encompassing very complex geometries in two or three dimensions. Fluent is capable of obtaining either steady state or transient solutions to problems involving a variety of flow phenomena, including flow in porous media. Fluent may also be expanded using user defined functions (UDFs) in order to add or modify closure relations and incorporate custom boundary conditions. Because CFD models such as Fluent solve the governing conservation equations throughout the model domain, they do not include some of the simplifying approximations and assumptions which are present in dedicated PTR models, and therefore there may be more confidence about their applicability to miniature systems. CFD models are also able to predict the complex flow details overlooked by one-dimensional models, likely improving their accuracy for miniature PTRs. For these reasons, CFD simulation is likely to be a very useful technique for modeling miniature PTRs.

There are limitations, however, that come along with the advantages of CFD modeling. The increased detail provided by CFD models is paid for with greatly increased computational time, and thus performing extensive parametric studies or geometry optimization with CFD may be prohibitively time consuming. To address this deficiency, the Sage[7] PTC modeling program was used for some preliminary optimization of the miniature PTR model geometry and operating conditions,

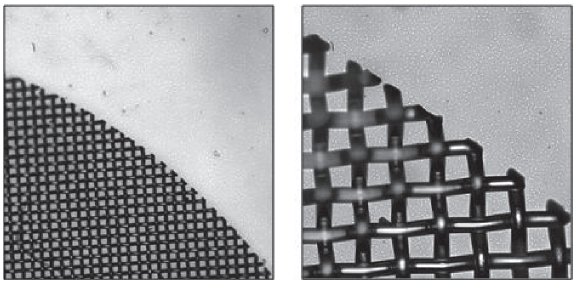

Figure 1. Magnified photographs of punched #635 stainless steel mesh screens.

particularly the determination of the inertance tube length. Sage is a widely used cryocooler model and design tool incorporating component level models which can be assembled to represent almost any Stirling or pulse tube cryocooler system. It is capable of very quickly solving for the steady-periodic performance of PTRs and performing multidimensional optimization of the many input variables to its component models. Sage does not solve for time-dependent behavior, however, and instead addresses the final steady-periodic operation. It is also one-dimensional, although it does include empirical corrections for some specific multidimensional effects. For larger scale systems, Sage has proven to be reliable and fairly accurate, particularly when its empirical corrections are based on directly relevant experimental results.

Parallel use of Sage and Fluent to model miniature PTCs has been previously demonstrated and described in detail[1]. The current work attempts to demonstrate the application of these models to a problem likely to be encountered in the miniaturization of these cryocoolers, with emphasis on the Fluent CFD models. Miniature PTCs with annular defects of ½ and 1 mesh screen pore diameter were modeled in Fluent and the effects of the gaps were determined qualitatively and quantitatively.

MINIATURE PTC MODELS

To model the effects of an open annular gap at the edge of a mesh screen regenerator, FLUENT models of a miniaturized PTC were constructed. A basic schematic of these models is shown in Figure 2, including detail views of the regenerator defect and the outline of the enlarged views shown later in Figures 7 and 8. The defect is an annular gap of width δ. Simulations were performed with defects of δ = 20 μm, 10 μm, and 0 μm. The regenerator filler was made of #635 stainless steel mesh which has a pore size of 20 μm. Therefore, the 10 and 20 μm defects corresponded to gaps of 0.5 and 1 mesh cell, respectively, while the 0 mm case or base model represented a perfectly filled regenerator.

Detailed geometry and operating conditions for the miniature PTC models are shown in Table 1. Much of the geometry was loosely based on our previous work[1] but some additional preliminary modeling was done using Sage, particularly the determination of a reasonable inertance line length. Significant geometry optimization in Fluent is difficult and computationally expensive; therefore, the parallel use of Sage can greatly expedite model development. It is important to note, however, that due to inherent differences between the two models the optimal inertance line lengths predicted by Sage are unlikely to be the best possible lengths for the CFD models.

The FLUENT models were two dimensional axisymetric representations of the entire PTC, with ideal-gas helium specified as their working fluid. The compressor was modeled with a moving wall and a dynamic meshing scheme which added and subtracted mesh layers as the wall moved. A user-defined sinusoidal displacement with a frequency of 200 Hz was applied to the moving compressor wall, shown with a double ended arrow in Figure 1, resulting in a pressure ratio at the

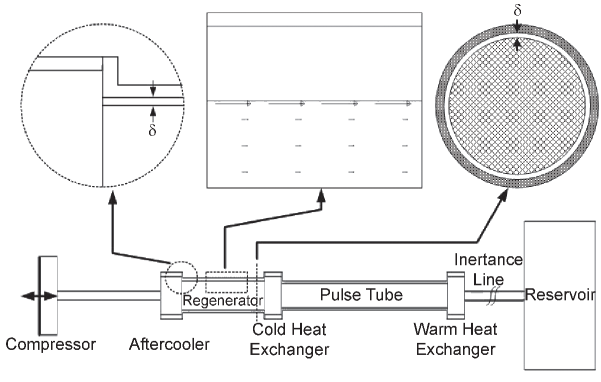

Figure 2. Schematic of PTR model with detail views.

Table 1. CFD model geometry and operating conditions.

Regenerator		Pulse Tube		Inertance Tube		Frequency	Operating
length (mm)	dia (mm)	length (mm)	dia (mm)	length (m)	dia (mm)	(Hz)	Pressure (MPa)
20	3	40	2.5	0.8208	1	200	4

Cold Heat Exchanger		Warm Heat Exchanger 2		Warm Heat Exchanger 1		Reservoir	Approximate Total
length (mm)	dia (mm)	length (mm)	dia (mm)	length (mm)	dia (mm)	Volume (cm^3)	Volume (cm^3)
4	4	4	4	5	4	5	6.3

transfer line inlet of approximately 1.25. In Fluent simulations 'PRESTO!' pressure discretization was used along with 'PISO' pressure-velocity coupling and second order upwind discretization of all other quantities; these settings were chosen to provide the best and fastest convergence of the models. Double precision, pressure-based steady and unsteady solvers were used with the physical velocity porous media flow formulation. Simulation results suggested that oscillatory turbulent flow might occur in the transfer and inertance lines; therefore, the standard k-omega turbulence model with low Reynolds number corrections was utilized. This turbulence model was chosen for its ability to handle transitionally turbulent flow and because it improved the convergence of the models. Residual convergence criteria were set at 10^{-9} for the energy equation and 10^{-8} for continuity, velocity, k, and omega.

Materials were selected for the models based upon their suitability for the fabrication of miniature PTCs. As stated above, #635 stainless steel mesh was chosen for the regenerator, while the aftercooler, warm and cold heat exchangers were all modeled as #325 phosphor-bronze mesh. These mesh fillers were selected for their small pore sizes and ability to be cut into discs small enough for the modeled PTCs. To model these materials, the FLUENT porous media model requires viscous and inertial resistance coefficients related to the Darcy permeability and Forchheimer's inertial coefficient. These parameters have been published for stacked screens of #635 stainless steel and #325 phosphor bronze mesh at 63% and 67% porosity, respectively, and are shown in Table 2[11].

The aftercooler, cold and warm heat exchanger walls were modeled as silver with wall thicknesses of 0.4 mm. The regenerator and pulse tube walls were modeled as stainless steel with a thickness of 0.28 mm. Wall conduction in these components was incorporated into the CFD models by discretizing the solid regions and applying the appropriate material properties. The outer surfaces of the aftercooler and warm heat exchanger walls were modeled isothermally at 293 K. The outside of the cold heat exchanger wall was also modeled isothermally at the various cold temperatures required for the load curve plots. The outer surfaces of the regenerator and pulse tube walls were modeled as adiabatic. The reservoir, inertance line, and the transfer line between the compressor and aftercooler were all modeled with isothermal walls at 293 K. Modeling wall thicknesses for these components was not necessary because the isothermal boundary condition eliminates axial temperature gradients rendering axial heat conduction negligible in their walls.

RESULTS

Simulations were performed across a range of temperatures for the base model (0 μm annular gap), 10 μm, and 20 μm gap models so that charts could be made of simulated net heat lift, phase angle, and specific power vs. temperature. Detailed 2-D plots of simulated velocity and temperature distributions in the region of the annular gap were also constructed for a few of the simulations. It

Table 2. Hydrodynamic parameters of modeled porous fillers.

Porous Media	Axial Direction		Radial Direction	
	Viscous Resistance $1/m^2$	Inertial Resistance 1/m	Viscous Resistance $1/m^2$	Inertial Resistance 1/m
# 325 Phosphor Bronze Mesh Screens	1.70E+10	50000	2.90E+10	50000
# 635 Stainless Steel Mesh Screens	9.50E+10	40000	1.11E+11	120000

was fastest and most efficient to use individual models for each temperature and annular gap, despite the large number of models required.

Each of these models was initialized with an approximate temperature distribution by iterating with the steady solver before beginning the transient simulation. This set up linear temperature gradients in the regenerator and pulse tube between the isothermal exterior wall temperatures of the aftercooler or warm heat exchanger and the cold heat exchanger. The first-order implicit transient solver was then used to iterate the models until they approached periodic steady state, at which point the model results would repeat for subsequent periods of the compressor oscillation. A time step of 20 μs was used, corresponding to 250 time steps per period of the 200 Hz operating frequency

A time history of the various energy fluxes into and out of a typical model is shown in Figure 3. All quantities are cycle-averaged using a moving window of 250 time steps, so they represent the average rates of heat or energy transfer into and out of the model. The inlet power is calculated from the flow rate of Fluent's 'total enthalpy' field variable at the junction of the compressor and transfer line. Similarly, the net heat fluxes for the aftercooler and heat exchangers are integrals of 'total surface heat flux'. For simplicity in reporting results, the aftercooler heat flux includes the heat transferred through the isothermal transfer line wall and the warm heat exchanger heat flux includes contributions from the inertance line and reservoir walls. The figure shows that the model converges rather quickly towards periodic steady state.

From the set of models previously described, simulated load curves of net heat lift vs. temperature were constructed and are shown in Figure 4. Each point is the predicted cycle-averaged heat

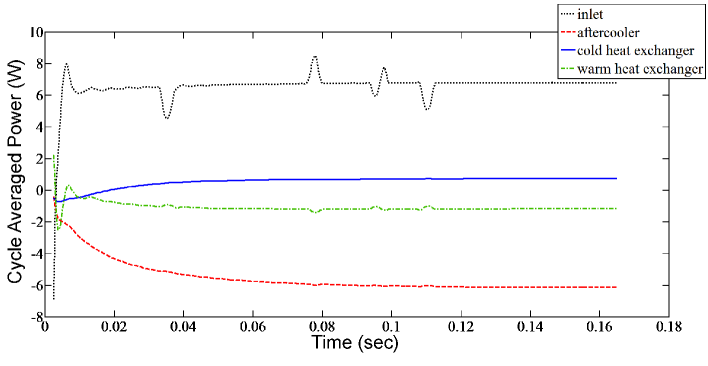

Figure 3. Sample model energy flux history, cycle averaged, for the base model at 180 K cold tip temperature.

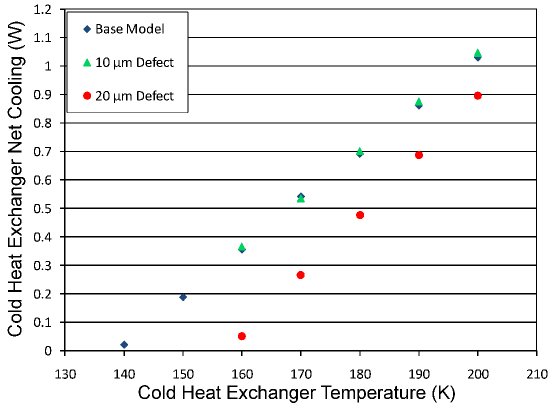

Figure 4. Simulated load curves.

flux through the cold heat exchanger exterior wall, which is modeled with an isothermal boundary condition at the temperature on the horizontal axis. Model results were all evaluated at 0.09 seconds of simulation time. The load curves show that the 10 µm regenerator defect is predicted to have very little effect on the net cooling. The 20 µm gap, however, significantly decreases the predicted performance and increases the predicted no-load temperature by approximately 20 K.

The annular regenerator gaps also affected the predicted phase difference between the pressure and velocity oscillations in the PTC. Figure 5 shows the predicted phase angle between pressure and velocity at the junction between the cold heat exchanger and the pulse tube. The positive phase angle corresponds to the pressure oscillation leading that of the velocity. There was some slight variation in the predicted phase angles with temperature, but generally the phase angle depended more on the size of the annular gap and decreased as the gap increased. The 10 µm defect had only a small effect while that of the 20 µm defect was much more pronounced. The dependence of the phase angle on the defects is actually secondary to its dependence on the inertance line length, which for these models was determined using Sage instead of Fluent. As was previously mentioned it is unlikely that the inertance length and phase angle of the base model are exactly optimized; therefore, the ultimate effect of the shift in phase angle caused by the defects on the overall performance predictions of the PTC model cannot be determined without additional modeling.

The effect of the regenerator defects on the efficiency of the simulated PTCs was determined from the specific power, defined as the ratio of input power to net heat lift. Figure 6 shows predicted curves of specific power versus cold heat exchanger temperature for the various models, with a

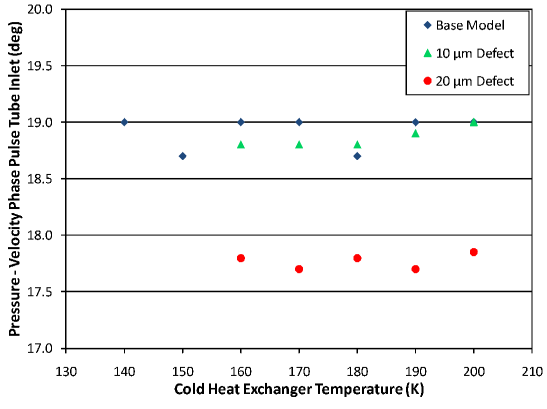

Figure 5. Simulated phase angle at the cold heat exchanger outlet.

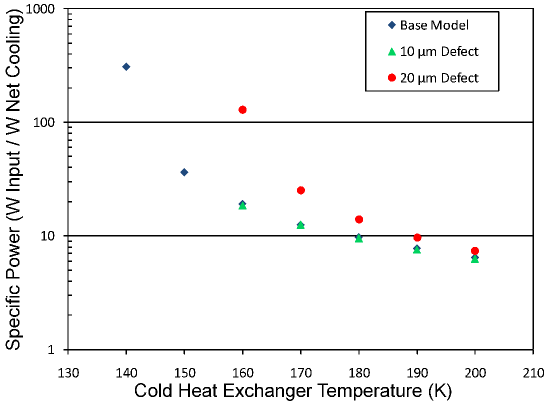

Figure 6. Simulated specific power.

logarithmic scale used on the vertical axis. As was the case in the net heat lift and phase angle plots, the 10 μm defect had little effect on the specific power. Again, the effect of the 20 μm defect was much more pronounced and increased the predicted specific power significantly, indicating a drop in the efficiency of the PTC model.

The curves in the previous three figures demonstrate the effects of the regenerator gaps on cycle-averaged quantities which describe the overall PTC model performance. They offer very little insight, however, into how the presence of the defects alters the physical processes occurring in the regenerator. One of the greatest advantages of CFD modeling, in comparison to other techniques, is the level of detail available in the model results. In the following figures, visualizations of the predicted instantaneous temperature and velocity fields illustrate the effects of the regenerator gaps on the thermal and hydrodynamic processes in the regenerator, providing some explanation for the effects seen on the predicted overall performance.

Figures 7 and 8 show instantaneous contours of axial velocity and temperature, respectively, for a small region near the regenerator wall, outlined in Figure 2. Both figures display model results at 0.1105 seconds of simulation time, at which point the velocity in the regenerator is at its cyclical maximum. Figure 7 shows that the effect of the open annular defects is to allow a higher velocity leakage of helium through the gaps around the regenerator. As would be expected, the width of this flow and its maximum velocity are both higher for the 20 μm gap (C) than the 10 μm (B). Figure 8 shows that the flow through the annular gap is warmer than that in the interior of the regenerator at the same axial position. Again the effect is more pronounced for the 20 μm gap, with significantly more penetration of warm gas into the colder end of the regenerator. At the opposite point in the cycle, not shown here, the maximum velocity in the other direction occurs; at this point the velocity and tem-

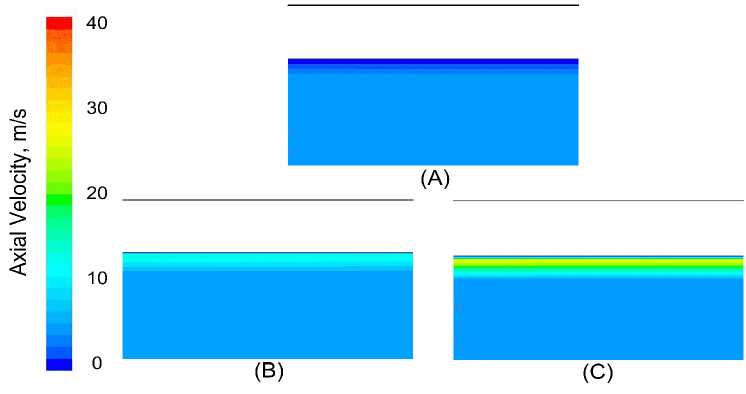

Figure 7. Velocity contours near the regenerator wall for (A) the base model, (B) the 10 μm defect model, and (C) the 20 μm defect model, all with 180 K cold temperature.

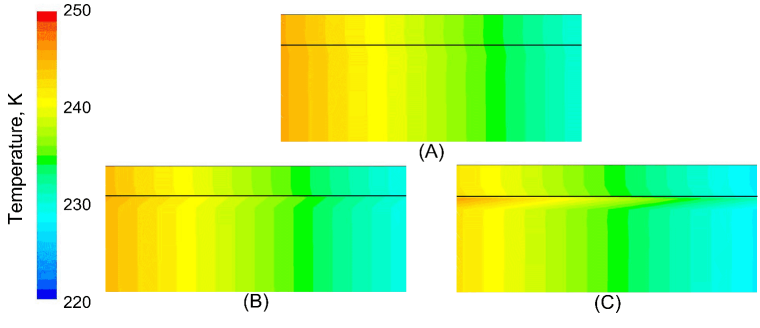

Figure 8. Temperature contours near the regenerator wall for (A) the base model, (B) the 10 mm defect model, and (C) the 20 mm defect model, all with 180 K cold temperature.

perature distributions are reversed and colder gas penetrates the warmer end of the regenerator. The temperature and velocity plots, considered together, confirm that the regenerator annular defect presents a lower resistance flow path around the regenerator which allows the working fluid to partially bypass it. This in turn would result in enhanced heat transfer from the warm end of the regenerator to the cold end, increasing the regenerator loss and reducing the net cooling power of the PTC.

DISCUSSION

The numerical results clearly indicate that the size of the gap between the edge of the regenerator matrix core and the inside of the regenerator shell is a critical parameter. The working fluid that bypasses the core and passes through the gap is not regenerated, resulting in a direct shuttling loss. Of particular interest is the quantitative observation that the magnitude of this shuttling loss increases dramatically somewhere between the defect gap sizes corresponding to ½ pore diameter and 1 full pore diameter. Wire mesh screens for stacked regenerators are generally manufactured by precision punching or electron discharge machining (EDM) the raw stock, in this case #635 mesh stainless steel filter cloth. As shown in Figure 1, the edge of a cut screen is not going to be defined by a solid wire, but rather by a series of partial cells with characteristic dimensions between 0 and 1 pore diameter. Therefore, to effectively achieve a defect gap on the order of ½ pore diameter, line-to-line contact between the regenerator screen outer diameter and the shell is practically required.

Unfortunately, this is difficult to accomplish. Aggressive but achievable machining tolerances on the diameter of the cut screens by either EDM or precision punch are on the order of +/- 13 microns (approximately +/- 0.5 mils). The regenerator shell inner diameter can be held somewhat tighter, but not without adding machining and inspection cost. What one finds, in short, is that the relevant manufacturing tolerances are precisely on the order of the tolerance to which this gap parameter must be controlled. Therefore, these results teach immediately that the proper manufacturing tolerance of the wire mesh-based regenerator components, screens and shell, is critical. Furthermore, the assembly of its components into an effectively zero-gap regenerator is also critical. Ultimately, this modeling result and the associated manufacturing assessment point towards the desirability of a completely different regenerator design, one in which this gap can either be eliminated by design or significantly better controlled.

CONCLUSIONS

Simulations of miniature pulse tube refrigerators with open annular gaps of 10 and 20 μm at the regenerator wall, as well as a baseline case with no gap, were performed using Fluent CFD software. These models represented imperfectly packed mesh screen regenerators with wall gaps of ½ and 1 pore diameter, respectively, of #635 stainless steel mesh which is commonly used as a regenerator filler in miniature PTCs. Simulated load curves of net heat lift vs. cold heat exchanger temperature were constructed to show the effect of regenerator defects on the overall PTR system performance. Visualizations of the velocity and temperature fields near the defect were also reported to illustrate the effects of the regenerator gaps on the thermal and hydrodynamic processes in the regenerator. The model results indicated that miniature PTRs may be quite tolerant of small annular defects in regenerator packing, but larger defects are likely to significantly reduce their performance. The results also demonstrated the capability of CFD to simulate a very small two dimensional detail which might be difficult or impossible to model using other techniques.

REFERENCES

1. Conrad, T.J., Landrum, E.C.,Ghiaasiaan, S.M., Kirkconnell, C.S.,Crittenden, T., Yorish, S., “CFD Modeling of Meso-Scale and Micro-Scale Pulse Tube Refrigerators,” *Cryocoolers 15*, ICC Press, Boulder, CO (2009), pp. 241-249.

2. Peterson, R.B., “Size limits for regenerative heat engines,” *Microscale Thermophysical Engineering,* Vol. 2, (1998) pp. 121-131.

3. Radebaugh, R., O'Gallagher, A., "Regenerator Operation at Very High Frequencies for Microcryocoolers," *Adv. in Cryogenic Engineering*, Vol. 51, Amer. Institute of Physics, Melville, NY (2006), pp. 1919-1928.

4. Bailly, Y., Nika, P., "Miniature Pulse Tube for the Cooling of Electronic Devices: Functioning Principles and Practical Modeling," *Microscale Thermophysical Engineering*, Vol 8, (2004) pp. 301-325.

5. Garaway, I., Gan, Z., Bradley, P., Radebaugh, R., "Development of a Miniature 150 Hz Pulse Tube Cryocooler," *Cryocoolers 15*, ICC Press, Boulder, CO (2009), pp. 105-113.

6. Ju, Y.L., Wang, C., Zhou, Y., "Numerical Simulation and Experimental Verification of the Oscillating Flow in Pulse Tube Refrigerator," *Cryogenics*, Vol 38 Issue 2, February 1998, pp. 169-176.

7. Gideon, D.,"Sage: Pulse Tube Model Class Reference Guide" (1999), Gideon Associates.

8. Fluent 6.3 User Guide, Fluent Inc. (2006).

9. Cha, J.S., Ghiaasiaan, S.M., Desai, P.V., Harvey, J.P., Kirkconnell, C.S., "Multi-Dimensional Effects in Pulse Tube Refrigerators," *Cryogenics*, Vol 46, Issue 9, September 2006, pp. 658-665.

10. Taylor, R.P., Nellis, G.F., Klein S.A., "Optimal Pulse-Tube Design Using Computational Fluid Dynamics," *Adv. in Cryogenic Engineering*, Vol. 51, Amer. Institute of Physics, Melville, NY (2006), pp. 1445-1453.

11. Conrad, T.J., Landrum, E.C., Ghiaasiaan, S.M., Kirkconnell, C.S., Crittenden, T., Yorish, S., "Anisotropic Hydrodynamic Parameters of Regenerator Materials Suitable for Miniature Cryocoolers," *Cryocoolers 15*, ICC Press, Boulder, CO (2009), pp. 343-351.